How to cite: *Angew. Chem. Int. Ed.* **2023**, *62*, e202215650
International Edition: doi.org/10.1002/anie.202215650
German Edition: doi.org/10.1002/ange.202215650

Supramolecular Chemistry

Diantimony Complexes $[Cp^R{}_2Mo_2(CO)_4(\mu,\eta^2\text{-}Sb_2)]$ ($Cp^R = C_5H_5$, $C_5H_4{}^tBu$) as Unexpected Ligands Stabilizing Silver(I)$_n$ ($n = 1$–4) Monomers, Dimers and Chains

*Pavel A. Shelyganov[+], Mehdi Elsayed Moussa[+], Michael Seidl, and Manfred Scheer**

Dedicated to Professor Rainer Streubel on the occasion of his 65th birthday

Abstract: Synthesis and reactivity of transition metal compounds bearing "naked" pnictogen atoms is an active research area with remarkable bonding patterns observed in the formed compounds. Within this field, intense investigations on the coordination behavior of complexes possessing P_n and As_n ($2 \le n \le 5$) moieties have been conducted. However, studies on heavier analogues have been ignored so far due to arduous challenges related to low yields and moderate air stability. Herein, we present the first in-depth study addressing the reactivity of organometallic complexes containing Sb-donor atoms with several Ag^I salts. These reactions afforded twelve unprecedented aggregates as monomers, dimers as well as three- and four-membered chains of Ag^I ions claimed in the literature to be inaccessible. Interatomic distances as well as computational evidence obtained with help of several different methods suggest the presence of Ag···Ag interactions in all complexes containing more than one Ag^I ion.

Introduction

Metal-directed self-assembly has become a powerful tool for the design of well-defined solid-state structures over the past decades.[1] In this field, aggregates assembled from Ag^I ions and multitopic organic molecules are especially attractive due to many special features and the range of emerging applications of Ag^I chemistry.[2] One common feature is closed-shell d^{10} argentophilic interactions which usually, similar to other metallophilic interactions,[3] brings small units together into intriguing supramolecular assemblies with captivating properties.[4] Another characteristic is the flexible coordination sphere of the Ag^I ion, which allows for the vast structural diversity of supramolecular compounds.[5] However, such flexibility challenges a selective and predictable synthesis[6] which renders it a less commonly used metal center in this field compared to other metal ions with well-defined coordination geometries (e.g: Pd^{II}, Pt^{II} and Au^I) displaying directed and predictable coordination angles.[1d–f] Typically, most of the Ag^I-based supramolecules are constructed from multitopic organic molecules bearing N-, O-, or P- and, to a lesser extent, S-, As- and C-donor atoms.[2,5,7] On the contrary, organometallic ligands have only rarely been used as building blocks for the synthesis of Ag^I supramolecular compounds.[8] To fill this gap, our group developed the concept of using organometallic polyphosphorus (P_n) ($n = 2$–6) and polyarsenic (As_n) ($n = 2$–3, 5) ligand complexes as ligands for Ag^I and other metal ions.[9] This concept allowed for the synthesis of a novel class of supramolecular assemblies including discrete supramolecular coordination complexes (SCCs) (monomers,[9a,b] dimers,[9b,c,e,10] oligomers,[9c] inorganic fullerene-like nanospheres,[11] nanosized hemispheres[12] and capsules[13]) as well as 1D, 2D and even 3D coordination polymers (CPs).[10a,14] Among the simplest P_n and As_n compounds are the diphosphorus and diarsenic ligand complexes $[Cp_2Mo_2(CO)_4(\eta^2\text{-}E_2)]$ (E = P (**A**),[15] As (**B**),[16] $Cp = C_5H_5$). The coordination chemistry of these complexes was thoroughly investigated in the past decade, mainly due to their ease accessibility, relative air stability and adaptive coordination modes.[9a,c,d,17] In contrary, synthesis and supramolecular chemistry studies of higher analogues such as the diantimony complex $[Cp_2Mo_2(CO)_4(\mu,\eta^2\text{-}Sb_2)]$ (**C**)[18] was, until recently, nearly ignored.[19] Roesler et al. studied the reactivity of **C** towards Ag^I and Cu^I metal ions (Scheme 1, **I**–**IV**) and suggested that **C** was an unsuitable ligand for coordination reactions towards Ag^I ions due to its rapid oxidation, which was supported by cyclic voltammetry and the reduction of the Ag^I ions to metallic silver by **C**.[19b] In fact, Ag^I complexes stabilized by any polyantimony ligand are extremely rare and limited to complexes bearing anionic tetra- or hexaantimony $\{Sb_n(C_6H_5)_n\}$ ($n = 4$, 6) chains or the neutral $O\{(CH_2)_2SbPh_2\}_2$ ligand (Scheme 1, **VI**).[20] Regarding polyantimony linkers supporting metallophilic interactions of any transition metal ion, to the best of our

[*] P. A. Shelyganov,[+] Dr. M. Elsayed Moussa,[+] Dr. M. Seidl, Prof. Dr. M. Scheer
Institute of Inorganic Chemistry, University of Regensburg
93040 Regensburg (Germany)
E-mail: manfred.scheer@chemie.uni-regensburg.de

[+] These authors contributed equally to this work.

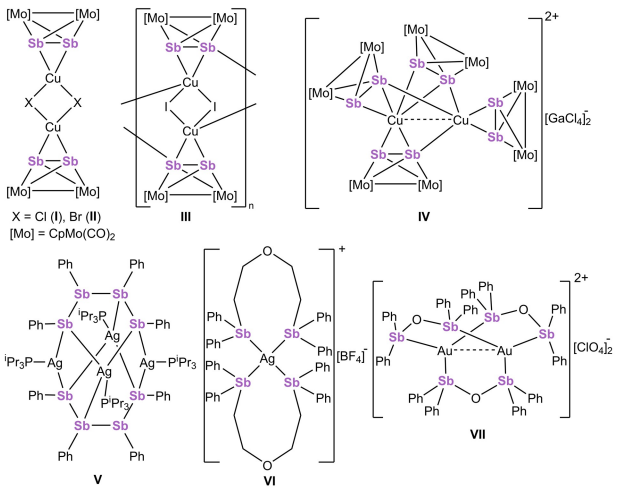

Scheme 1. Overview of the previously reported complexes bearing di- or polytopic antimony-based ligands. Adapted from ref. [18] (**I–IV**), [19] (**V–VI**) and [20] (**VII**).

knowledge, the only example is the Au^I dimeric paddle-wheel complex $[Au_2\{(Ph_2Sb)_2O\}_3][ClO_4]_2$ (Scheme 1, **VII**) featuring three ditopic Sb-donor ligands.[21] Recently, our group developed a general and effective approach for the synthesis of both homo- and heterodipnictogen ligand complexes $[Cp_2Mo_2(CO)_4(\mu,\eta^2\text{-}E_2)]$ and $[Cp_2Mo_2(CO)_4(\mu,\eta^2\text{-}EE')]$ ($E \neq E' = P$, As, Sb, Bi) on a gram scale[22] which opened the door to a deeper investigation of their reactivities.[23] Due to the fact that the chemistry of stibine ligands is in general much less developed than that of the lighter Group 15 analogs, and, due to literature evidence, demonstrating major differences in their coordination chemistry,[20b,24] we targeted to investigate the supramolecular chemistry of **C** towards transition metal ions.

In fact, we believed that optimizing the reaction conditions of **C** with Ag^I salts can probably lead to coordination processes, avoid oxidation and give rise to unprecedented supramolecular compounds of Ag^I and **C**. Herein we present a systematic study of reactions of **C** with a number of Ag^I salts (Ag[TEF], Ag[FAl], $Ag[SO_3CF_3]$ (Ag[OTf]), $Ag[PF_6]$ and $Ag[BF_4]$) using variable stoichiometries. These reactions result in the SCCs $[Ag(\eta^2\text{-}\mathbf{C})_3][X]$ ([X] = [TEF] (**1**), [FAl]- (**4**)), $[Ag_2(\eta^2\text{-}\mathbf{C})(\eta^{2:1}\text{-}\mathbf{C})_3][X]_2$ ([X] = [TEF] (**2**), [FAl] (**5**), $[PF_6]$ (**7**), [OTf] (**8**), $[BF_4]$ (**9**)), $[Ag_3(\eta^{1:2:1}\text{-}\mathbf{C})_3(\eta^{2:1}\text{-}\mathbf{C})_2][BF_4]_3$ (**10**), $[Ag_4(\eta^{1:2:1}\text{-}\mathbf{C})_2(\eta^{2:1}\text{-}\mathbf{C})_4][TEF]_4$ (**3**) and $[Ag_4(\eta^{1:2:1}\text{-}\mathbf{C})_2(\eta^{2:1}\text{-}\mathbf{C})_2(\eta^2\text{-}\mathbf{C})_2][FAl]$ (**6**). This synthetic approach was additionally extended by reacting Ag[TEF] with the tert-butyl-substituted derivative of **C**, $[(\eta^5\text{-}C_5H_4{}^t\text{Bu})_2Mo_2(CO)_4(\mu,\eta^2\text{-}Sb_2)]$ (**C′**), to give the SCCs $[Ag(\eta^2\text{-}\mathbf{C'})_3][TEF]$ (**11**) and $[Ag_2(\eta^2\text{-}\mathbf{C'})(\eta^{2:1}\text{-}\mathbf{C'})_3][TEF]_2$ (**12**). The Ag···Ag contacts which are present in the SCCs **2**, **3**, **5**–**10** and **12** were attributed to argentophilic interactions according to DFT calculations. This study is the first and only in-depth study having been conducted for the reaction of Ag^I ions with any diantimony ligand, and the formed Ag^I SCCs **1**–**12** are unique and very challenging examples in the field of Ag^I-based coordination compounds due to the high sensitivity of **C** towards oxidation in the presence of Ag^I ions.

Results and Discussion

In a first step, the ligand complex **C** was treated with Ag[TEF] due to the high solubility of the $[TEF]^-$ salts. This reaction was carried out in CH_2Cl_2 at room temperature by slow addition of a solution of Ag[TEF] to that of **C** (Scheme 2a). Depending on the ratio $\mathbf{C}:Ag^I$ used (3:1 and 2:1), compounds **1** (83 % yield) and **2** (65 % yield), respectively, could be isolated as red crystalline materials upon layering the crude reaction mixtures with *n*-pentane. The solid-state structure of **1** shows a monomeric SCC of the general formula $[Ag(\eta^2\text{-}\mathbf{C})_3][TEF]$ (Scheme 2a and b). Its Ag^I core is stabilized by three **C** ligands each possessing an η^2-coordination mode, thus the Ag^I ion in **1** possesses a distorted trigonal prismatic environment. In contrast to **1**, compound **2** crystalizes as a dicationic SCC of the general formula $[Ag_2(\eta^{2:1}\text{-}\mathbf{C})_3(\eta^2\text{-}\mathbf{C})][TEF]_2$ (Scheme 2a and c). The central structural motif of **2** consists of two Ag^I ions located only 2.884(1) Å apart, which is significantly shorter than the sum of their van der Waals radii (3.44 Å), revealing possible Ag···Ag interaction.[4e,25] Moreover, three of the ligands **C** found in **2** each show a bridging $\eta^{2:1}$-coordination mode and one ligand **C** exhibits a terminal η^2-coordination. Notably, all three bridging ligand complexes **C** are coordinated towards Ag1 through an η^1-coordination mode while they coordinate to Ag2 via the η^2-coordination mode. As a consequence, Ag1 is hexacoordinated by five Sb atoms and one Ag^I ion while Ag2 is heptacoordinated by six Sb atoms and one Ag^I ion. According to the CSD database,[26] **1** and **2** are the first SCCs in which an Ag^I ion is stabilized by five or six Sb atoms.

The reaction of **C** with Ag[TEF] in a $\mathbf{C}:Ag^I$ ratio of 1:1 in CH_2Cl_2 allowed upon layering with *n*-pentane the formation of dark brown precipitate. However, upon recrystallization from *o*-$C_6H_4F_2$ (*o*-DFB), compound **3** was isolated as red single crystals suitable for X-ray structure analysis (yield 57 %). The cationic part of the asymmetric unit contains the dicationic fragment $[Ag_2(\eta^{1:2:1}\text{-}\mathbf{C})(\eta^{2:1}\text{-}\mathbf{C})_2]$ which is duplicated due to an inversion center. Thus, the molecular structure of **3** reveals a tetracationic SCC of the general formula $[Ag_4(\eta^{1:2:1}\text{-}\mathbf{C})_2(\eta^{2:1}\text{-}\mathbf{C})_4][TEF]_4$ (Scheme 2a and d). Remarkably, the core of **3** is composed of four Ag^I ions located in close proximity (d(Ag···Ag) = 2.836(1)–2.869 (2) Å) thus forming a tetrameric silver chain. Additionally, the per-atom RMSD of the best straight-line for the Ag^I ions in **3** is as small as 0.123 Å, revealing that the tetrameric silver chain is nearly linear with only a slight zig-zag distortion. The four-membered silver chain in **3** is stabilized by six ligand complexes **C** in which four of them each adopt an $\eta^{2:1}$-coordination mode while each of the other two possess an $\eta^{1:2:1}$-coordination. Interestingly, the $\eta^{1:2:1}$-coordinated ligands each link three adjacent Ag^I centers while the $\eta^{2:1}$-coordinated ones each connect two adjacent Ag^I ions. The Sb–Sb bonds in **1** (2.722(1)–2.743(1) Å), **2** (2.745(1)–2.778(1) Å) and **3** (2.770(1)–2.776(1) Å) are slightly elon-

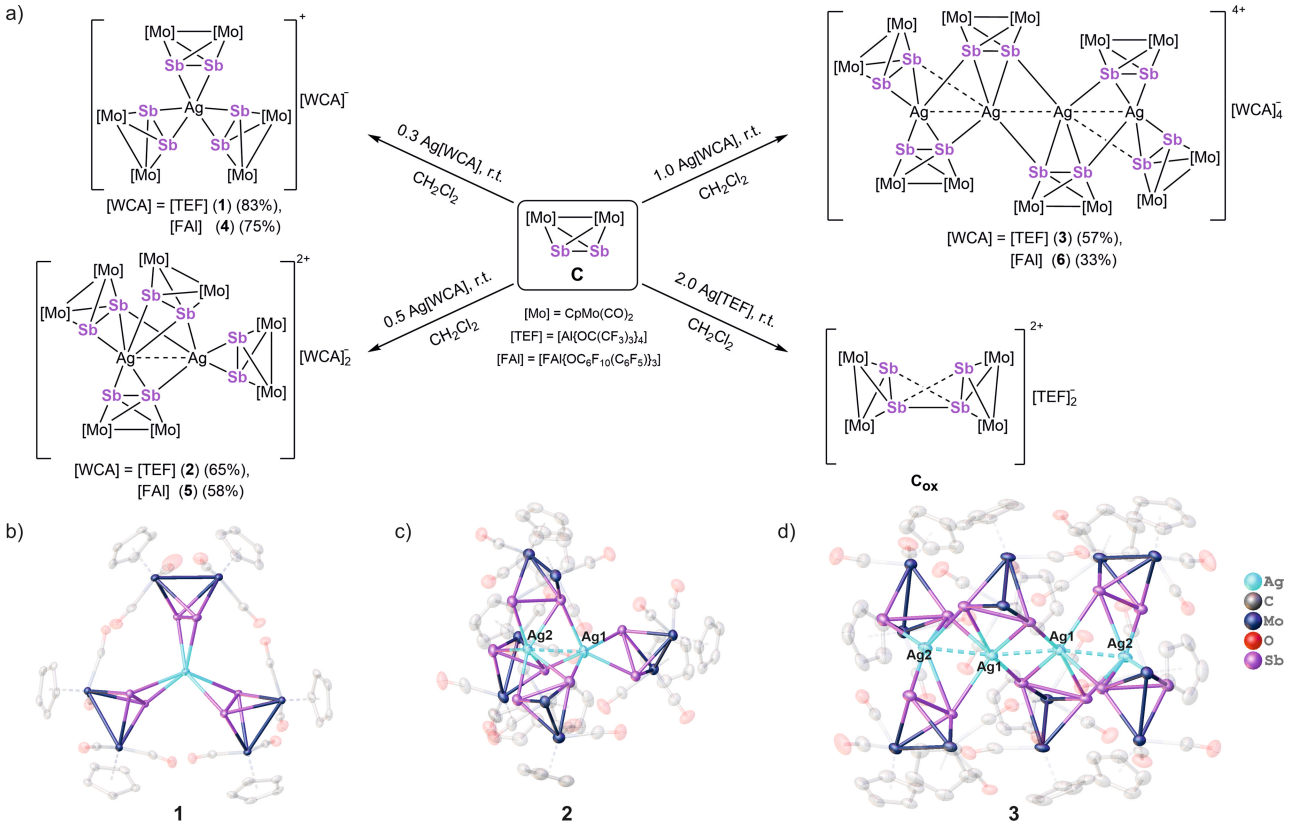

Scheme 2. a) Reactions of **C** with Ag[TEF] and Ag[FAl] with a variety of **C**:Ag^{I} stoichiometries. Synthesis of SCCs **1**–**6**. Yields are given in parentheses; Solid state structure of SCCs b) **1** (**4** has a similar structure), c) **2** (**5** has a similar structure) and d) **3** (structure of **6** is shown in detail in Figure S7 in the Supporting Information). Hydrogen atoms are omitted for clarity, Cp and CO ligands are faded out.

gated compared to that found in the non-coordinated ligand **C** (2.687(1) Å). The Ag–Sb bond lengths in **1**–**3** are in the range of 2.768(1)–3.148(1) Å which are comparable to those found in literature according to the CSD database (2.564(1)–3.128(1) Å).

The room temperature reaction of one equivalent of **C** with two equivalents of Ag[TEF] in CH_2Cl_2 resulted in an Ag^0 mirror which was observed at the walls of the reaction vessel together with the formation of the tetraantimony dicationic compound $[\{(C_5H_5)Mo(CO)_2\}_4\{\eta^{2:2:2:2}\text{-}Sb_4\}][TEF]_2$ (**C$_{ox}$**) previously reported as a product of the oxidation reaction of **C** with $[C_{12}H_8S_2][TEF]$.[23] Noteworthy, the oxidation was observed for both samples kept in the dark and exposed to daylight.

The isolation of **1**–**3** shows the accessibility of SCCs of Ag^{I} and **C** with various compositions. It is also shown that the undesired oxidation of **C** can be circumvented by avoiding an excess of the Ag^{I} salt, which also includes the slow addition of the Ag^{I} solution to a solution of **C**, preventing a local excess of Ag^{I}. The fact that **C** exhibits three different coordination modes (η^2, $\eta^{2:1}$, $\eta^{1:2:1}$) in **1**–**3** shows also its flexible coordination behavior and its capability of adaptive coordination within the formed SCCs.

In a second approach, the effect of changing the anion on the reaction outcome was studied by reacting **C** with Ag[FAl] as well as with several common Ag^{I} salts Ag[X] (X = $[PF_6]^-$, $[OTf]^-$ and $[BF_4]^-$). Similar to those conducted with Ag[TEF], reactions of **C** with Ag[FAl] were performed in CH_2Cl_2. Since the solubility of the $[FAl]^-$ anion is lower than that of $[TEF]^-$, in each reaction, one drop of CH_3CN was added to the reaction mixture to ensure the complete solubility of Ag[FAl]. The reactions with **C**:Ag^{I} in ratios of 3:1, 2:1 and 1:1 yielded compounds **4** (yield 75 %), **5** (yield 58 %) and **6** (yield 33 %), respectively (Scheme 2a). In line with the SCCs **1** and **2**, the molecular structures of **4** and **5** reveal mono- and dicationic SCCs $[Ag(\eta^2\text{-}\mathbf{C})_3][FAl]$ and $[Ag_2(\eta^{1:2}\text{-}\mathbf{C})_3(\eta^2\text{-}\mathbf{C})][FAl]_2$, respectively. The general structures of **4** and **5** including the coordination modes of **C**, the Sb–Sb and Ag–Sb bond lengths as well as Ag···Ag interatomic distances are similar to those observed in their $[TEF]^-$ analogs **1** and **2**. Similar to **3**, the solid-state structure of **6** shows a tetracationic compound, however, the four-membered chain of Ag^{I} ions in **6** is heavily disordered over at least three positions. Its major component (occupancy 0.44) shows the SCC $[Ag_4(\eta^{1:2:1}\text{-}\mathbf{C})_2(\eta^{2:1}\text{-}\mathbf{C})_2(\eta^2\text{-}\mathbf{C})_2]FAl]_4$.[27] In this structure, four Ag^{I} ions are surrounded by two $\eta^{1:2:1}$-coordinated, two η^2- and two $\eta^{2:1}$-coordinated complexes **C** (for a detailed description of the disorder in **6** see Supporting Information). In the reactions of the silver salts Ag[X] (X = $[PF_6]^-$, $[OTf]^-$ and $[BF_4]^-$) with **C**, a 2:1 CH_2Cl_2:CH_3CN solvent mixture was used due to their lower solubility compared to Ag[TEF] and Ag[FAl]. In contrast to similar reactions of **C** with Ag[TEF] and Ag[FAl], for every reaction with these Ag^{I} salts, both the 3:1 and the 2:1 ratio

reactions yielded selectively, upon layering the crude reaction mixture with *n*-pentane, products of the general formula $[Ag_2(\eta^{2:1}\text{-}\mathbf{C})_3(\eta^2\text{-}\mathbf{C})][X]_2$ ([X] = $[PF_6]^-$ (**7**, yield 35 %), $[OTf]^-$ (**8**, yield 53 %), $[BF_4]^-$ (**9**, yield 42 %)) (Scheme 3a, Figures S8–S10) analogous to the dimeric SCCs **2** and **5** (Scheme 2a). Similar to what was found in **2** and **5**, short Ag···Ag distances exist in the solid-state structures of **7**–**9** (2.828(1)–2.889(1) Å). The fact that no monomeric complexes $[Ag(\eta^2\text{-}\mathbf{C})_3][X]$ ([X] = $[PF_6]^-$, $[OTf]^-$, $[BF_4]^-$) similar to **1** and **4** were obtained from the 3:1 ratio reactions led to the question of whether this result is due to the change of the counterion or due to the change of the solvent used in the reactions. To address this issue, reactions of **C** with Ag[TEF] and Ag[FAl] with a 3:1 stoichiometry were reproduced in a 2:1 mixture of CH_2Cl_2 and CH_3CN (this solvent mixture corresponds to that used for the synthesis of **7**–**9**). Both reactions exclusively yielded monocationic SCCs (**1** and **4**, respectively) demonstrating that the reaction with a 3:1 **C**:Ag^I ratio is directed towards monomeric or dimeric products by the change of the Ag^I salt rather than by changing the solvent system. Remarkably, reactions of **C** with $Ag[PF_6]$ and Ag[OTf] in a 1:1 ratio still yield the dicationic SCCs **7** and **8**. On the contrary, the reaction of **C** with $Ag[BF_4]$ using a 1:1 stoichiometry led to a selective formation of the tricationic SCC of the formula $[Ag_3(\eta^2\text{-}\mathbf{C})_2(\eta^{1:2:1}\text{-}\mathbf{C})_3][BF_4]_3$ (**10**, yield 38 %) (Scheme 3a). Its cationic part shows an unprecedented chain of three Ag^I ions stabilized by five ligand complexes **C**. Three central complexes **C** each show a bridging $\eta^{1:2:1}$-coordination mode and link all three Ag^I ions together (Scheme 3b), while two other complexes **C** each possess an η^2-coordination stabilizing the terminal Ag1 and Ag3 ions, therefore acting as non-bridging ligands. The fact that the SCC possessing a 5:3 composition in $[Ag_3(\eta^2\text{-}\mathbf{C})_2(\eta^{1:2:1}\text{-}\mathbf{C})_3][BF_4]_3$ (**10**) is only accessible with $Ag[BF]_4$ additionally highlights that the anion has an effect on directing the reactions towards supramolecules having different solid-state structures.

To rationalize the coordination modes of **C** towards metal ions and compare them to those in the lighter phosphorus (**A**) and arsenic (**B**) analogs,[9c] Natural Bond Orbital (NBO) calculations were performed for compounds **A**–**C** at the B3LYP[28]/def2-TZVP[29] level of theory. These calculations show that the energy level of the Sb–Sb σ-bond in **C** is higher than that of the As–As σ-bond in **B**, which is, in turn, higher than that of the P–P σ-bond in **A**, showing a clear trend (Figure 1). Remarkably, the gap between the energy level of the σ-bond and the LP in **C** (3.91 eV) is significantly larger than that in **B** (2.85 eV) and much larger than that in **A** (0.55 eV), therefore the coordination through the Sb–Sb σ-bond in **C** is expected to be more favorable than the coordination through the LPs of the Sb atoms. The Bond Orders (BOs) of the σ(Sb–Sb) bonds of the units **C** in **1**–**10**[30] as well as that of the non-coordinated complex **C** (calculated using Density Derived Electrostatic and Chemical (DDEC)[31] approach[32] (BP86[33]/def2-SVP,[29] see Supporting Information for details) allow for the attribution of the η^2-coordination mode to the "through-bond" coordination. Likewise, the η^1-coordination mode was assigned to donation from the lone pair of Sb atom. Accordingly, $\eta^{2:1}$- and $\eta^{1:2:1}$-coordination modes can be seen as combinations of the η^2- with either one or two η^1-coordination modes. The di-(**2**, **5**, **7**–**9**), tri- (**10**) and tetracationic (**3**, **6**) SCCs contain Ag···Ag contacts that are shorter than the sum of the van der Waals radii (3.44 Å) indicating possible silver-silver interactions.

Our assumption of the presence of argentophilic interactions in SCCs **2**, **3**, **5**–**10** is based exclusively on interatomic distances and their relation to the sum of the van der Waals

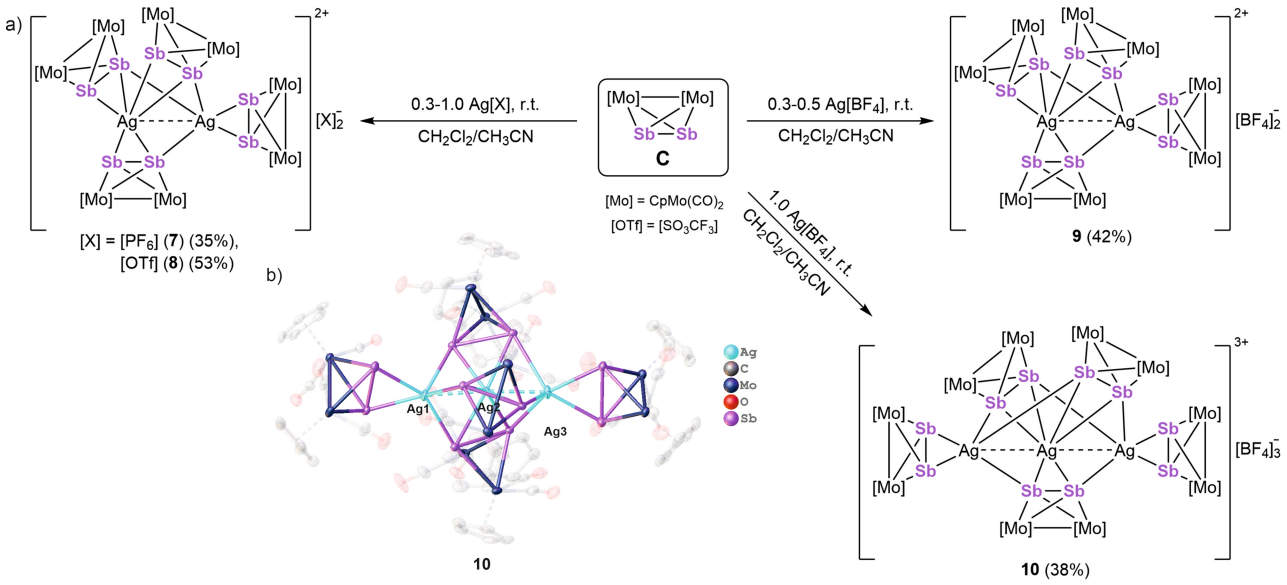

Scheme 3. a) Reactions of **C** with $Ag[PF_6]$ and Ag[OTf] with a variety of **C**:Ag^I stoichiometries. Synthesis of SCCs **7**–**10**. Yields are shown in parentheses; b) Solid-state structure of SCC **10** (one of three tricationic SCCs present in the asymmetric unit is shown). Hydrogen atoms are omitted for clarity, Cp and CO ligands are faded out.

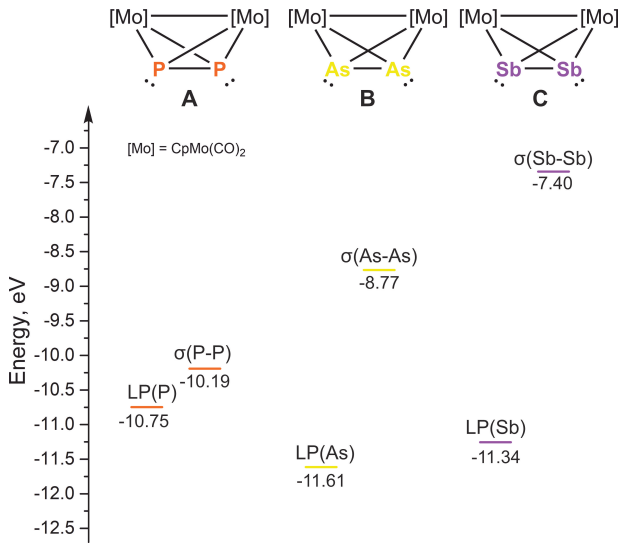

Figure 1. Natural Bonding Orbital (NBO) energy diagram of **A**–**C** calculated at the B3LYP/def2-TZVP level of theory. Calculations for **A**–**B** are adapted from the ref. [9c].

radii which is a criterion very commonly used in the literature.[4f,34] However, this approach is sometimes subjected to justified criticism as being oversimplified.[35] On the contrary, the Ag···Ag short contacts attributed to argentophilic interactions with supporting calculations seem more reliable.[7e,36] To shed more light on the presence of such interactions in the compounds **2**, **3**, **5**–**10**, BOs corresponding to short Ag···Ag contacts were calculated (DDEC approach, BP86/def2-SVP, for more information see Supporting Information). In di- (0.241), tri- (0.260–0.264) and tetracationic (0.222–0.256) SCCs, BOs of approx. 0.2 were attributed to the Ag···Ag short contacts. In addition, for these SCCs, the Interaction Region Indicators[37] (IRIs) were calculated using Multiwfn software.[38] For every compound, the visual analysis of the IRI surfaces also indicated the presence of attractive interactions between adjacent Ag^I ions (see Supporting Information (Figure S17) for details). Further, to shed light on interactions between neighboring Ag^I ions, the Extended-Transition-State Natural Orbitals for Chemical Valence[39] (ETS-NOCV) analysis has been performed for di- and trimeric SCCs. In each case the visual analysis of the most significant NOCV pairs shows the interaction between d_{z^2} orbitals of one Ag^I ion with hybrid orbitals of neighboring Ag^I centers leading to accumulation of electron density between these Ag^I ions, thus, indicating the presence of orbital interactions between them (Figure S22, for more details see Supporting Information). Finally, the Quantum Theory of Atom in Molecules (QTAIM) analysis[40] has been performed on these SCCs showing in each case the presence of (3,1) bond critical points between two neighboring Ag^I ions (see Supporting Information for details). These results support our initial assumption that argentophilic interactions supported by ligand complexes **C** are present in the SCCs **2**, **3**, **5**–**10**.

The SCCs **1**–**10** are well soluble in common organic solvents such as CH_2Cl_2 (**1**–**6**) and CH_3CN (**1**–**10**), little soluble in THF and toluene (**1**–**10**) and insoluble in *n*-pentane (**1**–**10**). The room temperature ^1H NMR spectra of **1**–**10** in CD_3CN show in each case one singlet in the range of 5.23–5.30 ppm which is attributed to protons of the Cp rings, and which are all slightly downfield shifted as compared to that of free **C** (5.19 ppm in CD_3CN). The heteronuclear ($^{19}F\{^1H\}$ (**1**–**10**), $^{11}B\{^1H\}$(**9**, **10**) and $^{31}P\{^1H\}$ (**7**)) NMR spectra of **1**–**10** in CD_3CN exhibit the expected characteristic signals of the corresponding anions (see Supporting Information for details). The fact that in the ^1H NMR spectra of the SCCs **1**–**10** only a single signal of the Cp protons is detected implies that they exhibit dynamic behavior in solution. Moreover, the variable temperature ^1H NMR spectrum in CD_2Cl_2 of **1** also shows only one sharp singlet between 5.06–5.15 ppm in the temperature range of 193–300 K suggesting that the exchange of non-coordinated and coordinated ligands **C** is fast in the NMR timescale in this temperature range.

In the electrospray ionization mass spectrometry (ESI-MS) spectra of **1**–**10** in CH_2Cl_2 or CH_3CN (see Supporting Information for details), the most abundant peak (100 %) is attributed to the $[Ag\mathbf{C}_2]^+$. Additionally, the peak corresponding to the $[Ag\mathbf{C}_3]^+$ moiety is observed for the monomeric complexes **1** (8 %) and **4** (13 %) suggesting they remain, at least partially, intact in solution. The ESI-MS spectra of tri- (**10**) and tetrameric (**3**, **6**) SCCs show peaks corresponding to fragments $[Ag\mathbf{C}]^+$ (67 % (**3**), 3 % (**6**), 49 % (**10**)) and $[Ag\mathbf{C}(CH_3CN)]^+$ (43 % (**3**), 2 % (**6**), 33 % (**10**)). Since CH_3CN ligands are rather labile, they can easily decoordinate an Ag^I ion upon ionization in the ESI-MS device, thus, we assume these two peaks do correspond to the same species $[Ag\mathbf{C}(CH_3CN)_x]^+$ in solution. Lastly, compounds **1**, **4**, **5**, **7**–**10** show in their ESI-MS spectra minor, yet observable peaks (0.1–1 %) attributed to the species $[\{Ag_2\mathbf{C}_3\}\{X\}]^+$ (X = [Cl]$^-$[41] (**1**, **4**, **5**), $[PF_6]^-$ (**7**), $[OTf]^-$ (**8**), $[BF_4]^-$ (**9** and **10**), while the ESI-MS spectrum of **10** shows an additional set of weak peaks corresponding to the fragments $[\{Ag_3\mathbf{C}_3\}\{Cl\}_2]^+$, $[\{Ag_3\mathbf{C}_3\}\{Cl\}\{BF_4\}]^+$ and $[\{Ag_3\mathbf{C}_3\}\{BF_4\}_2]^+$ ($\approx$0.1 % each).[42]

The fact that the main fragment observed in the ESI-MS from solutions of all compounds **1**–**10** is $[Ag\mathbf{C}_2]^+$ encouraged us to speculate about a mechanism for the formation of these SCCs. We assume that there is an equilibrium between $[Ag\mathbf{C}_3]^+$ and $[Ag\mathbf{C}_2]^+ + \mathbf{C}$ in solutions of **1** and **4** (Figure 2 a), but only compounds featuring three complexes **C** crystallize as products. The cationic part of the dimeric SCCs **2**, **5**, **7**–**9** is probably formed by the dimerization of two $[Ag\mathbf{C}_2]^+$ fragments together with corresponding changes in the coordination modes of **C** (Figure 2b). Similarly, the tri- (**10**) and tetracationic (**3**, **6**) cores of the SCCs **3**, **6** and **10** can be assembled upon proper re-organization of the coordination modes of **C**, from two $[Ag\mathbf{C}_2]^+$ moieties and either one or two $[Ag\mathbf{C}]^+$ fragments (Figure 2c and d).[43]

The solid-state IR spectra of the SCCs **1**–**10** each show two to four strong broad absorption bands in the range 1885 to 1991 cm^{-1} corresponding to the stretching vibrations of the CO ligands in the coordinated ligand complexes **C**. These absorptions appear at higher energies than those reported for the free complex **C** (1880 and 1916 cm^{-1}).

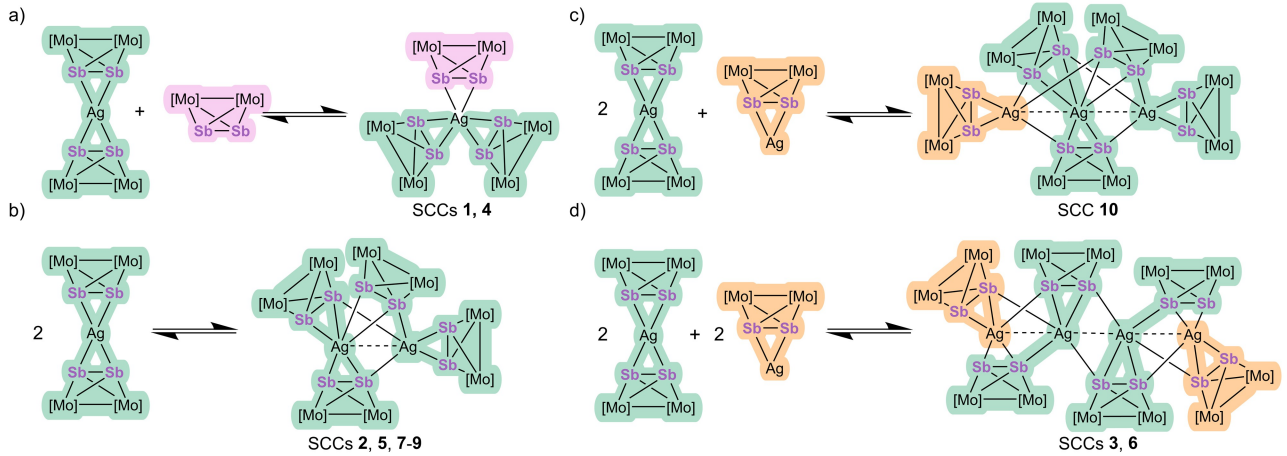

Figure 2. Suggested relations between species present in solutions of **1**–**10** and the SCCs **1**–**10**: a) $[Ag\mathbf{C}_2]^+$, **C**, $[Ag\mathbf{C}_3]^+$; b) $[Ag\mathbf{C}_2]^+$, $[Ag_2\mathbf{C}_4]^{2+}$; c) $[Ag\mathbf{C}_2]^+$, $[Ag\mathbf{C}]^+$, $[Ag_3\mathbf{C}_5]^{3+}$; d) $[Ag\mathbf{C}_2]^+$, $[Ag\mathbf{C}]^+$ and $[Ag_4\mathbf{C}_6]^{4+}$. The fragments $[Ag\mathbf{C}_2]^+$ (green), **C** (purple) and $[Ag\mathbf{C}]^+$ (orange) are highlighted in colors. Ag^I ion of the species $[Ag\mathbf{C}]^+$ are highly likely to coordinate to some solvent molecules in solution (not depicted). Charges are omitted for clarity.

The isolation of all SCCs **1**–**10** shows the feasibility of our approach upon varying Ag^I salts with various anion sizes and solubilities. Still, however, we were interested in further studying the effect of modifying the backbone of **C** on the products formed upon reaction with Ag[TEF]. To address this issue, we synthesized the *tert*-butyl-substituted analog of **C**, $[Cp'_2Mo_2(CO)_4(\eta^2\text{-}Sb_2)]$ (**C′**, $Cp' = C_5H_4{}^tBu$).[44] Under reaction conditions similar to those used for the synthesis of the SCCs **1**–**3**, **C′** was treated with Ag[TEF] using 3:1, 2:1 and 1:1 ratios of **C′**:Ag^I. The 3:1 reaction afforded the monocationic SCC $[Ag(\eta^2\text{-}\mathbf{C}')_3][TEF]$ (**11**, yield 67 %), while the 2:1 ratio reaction resulted in the dicationic complexes $[Ag_2(\eta^{2:1}\text{-}\mathbf{C}')_3(\eta^2\text{-}\mathbf{C}')][TEF]_2$ (**12**, yield 74 %). The molecular structures of **11** and **12** are similar to those of their analogs **1** and **2** (Figure S13 and S14). These results imply that the influence of the ^{t}Bu substituent at the Cp^R ligand (adding more solubility and further steric hindrance) on the formed supramolecular compounds is neglectable.

Conclusion

In summary, a unique class of Ag^I SCCs (**1**–**12**) was obtained using the tetrahedral diantimony complexes **C** or **C′** and a variety of Ag^I salts as building blocks under special conditions by avoiding the reduction to elemental Ag. Accordingly, mono-(**1**, **4**, **11**) and dimeric (**2**, **5**, **7**–**9**, **12**) aggregates as well as tri- (**10**) and even tetrameric (**3**, **6**) chain compounds have been isolated depending on the choice of the Ag^I salt and the reaction stoichiometry. Interestingly, Ag···Ag distances found in the X-ray structures, together with DFT calculations, suggest the presence of argentophilic interactions in all complexes containing more than one Ag^I ion. Furthermore, it is noticed that in the solid-state structures of **1**–**12**, complex **C** can adopt η^2-, $\eta^{2:1}$- and $\eta^{1:2:1}$-coordination modes or a mixture of two or all of them, reflecting its flexible and adaptive coordination behavior in supramolecular chemistry. These reactivity patterns of **C** towards Ag^I ions are more comparable to those found for its As-analog **B** $[Cp_2Mo_2(CO)_4(\eta^2\text{-}As_2)]$ rather than the P-analog **A**, but show, even in comparison to the As compound **B**, a much different coordination behavior as e.g. the formation of the four-membered Ag chain compounds **3** and **6**. According to DFT calculations, these reactivity differences towards metal ions arise from the relative energies of the pnictogen atoms lone pairs and the pnictogen-pnictogen sigma bonds. Specifically, the Sb–Sb σ-bond in **C** is more accessible for a coordination to metal centers than the As–As and especially P–P σ-bonds in **B** and **A**, respectively. Such σ-donation towards Ag^I ions, accompanied by the coordination potential of the Sb lone pairs, gives **C** an extraordinary flexibility and promotes the formation of both oligomeric assemblies featuring remarkable argentophilic interactions (**2**, **3**, **5**–**10**, **12**) and monomeric complexes (**1**, **4**, **11**). Finally, based on the data obtained from ESI-MS spectra in solutions of **1**–**12**, we were able to demonstrate a logic process for the aggregation reactions leading to the formation of the found structures in the solid-state. Current investigations in this field concentrate on extending this research area towards the even more sensitive Bi-analog $[Cp_2Mo_2(CO)_4(\eta^2\text{-}Bi_2)]$ as well as the heterodiatomic group 15 complexes $[Cp_2Mo_2(CO)_4(\eta^2\text{-}EE')]$ ($E \neq E' =$ As, Sb, Bi), a chemistry which had never been explored before.

The supplementary crystallographic data for this paper are provided free of charge by the joint Cambridge Crystallographic Data Centre and Fachinformationszentrum Karlsruhe Access Structure service.[45]

Acknowledgements

This work was supported by the Deutsche Forschungsgemeinschaft within the projects Sche 384/44-1 and Sche

384/42-1. Open Access funding enabled and organized by Projekt DEAL.

Conflict of Interest

The authors declare no conflict of interest.

Data Availability Statement

The data that support the findings of this study are available in the Supporting Information of this article.

Keywords: Antimony · Argentophilic Interactions · Self-Assembly · Silver · Weakly Coordination Anions

[1] a) T. L. Mako, J. M. Racicot, M. Levine, *Chem. Rev.* **2019**, *119*, 322–477; b) Y. Lu, H. N. Zhang, G. X. Jin, *Acc. Chem. Res.* **2018**, *51*, 2148–2158; c) M. M. Gan, J. Q. Liu, L. Zhan, Y. Y. Wang, F. E. Hahn, Y. F. Han, *Chem. Rev.* **2018**, *118*, 9587–9641; d) T. R. Cook, P. J. Stang, *Chem. Rev.* **2015**, *115*, 7001–7045; e) T. R. Cook, Y. R. Zheng, P. J. Stang, *Chem. Rev.* **2013**, *113*, 734–777; f) R. Chakrabarty, P. S. Mukherjee, P. J. Stang, *Chem. Rev.* **2011**, *111*, 6810–6918.

[2] a) X. X. Kong, Q. Q. Shen, T. T. Wan, K. Y. Li, F. G. Sun, H. L. Wu, *J. Chin. Chem. Soc.* **2022**, *69*, 540–548; b) K. Dammak, M. Porchia, M. De Franco, M. Zancato, H. Naili, V. Gandin, C. Marzano, *Molecules* **2020**, *25*, 5484; c) M. I. Rogovoy, D. G. Samsonenko, M. I. Rakhmanova, A. V. Artem'ev, *Inorg. Chim. Acta* **2019**, *489*, 19–26; d) J. M. Alderson, J. R. Corbin, J. M. Schomaker, *Acc. Chem. Res.* **2017**, *50*, 2147–2158; e) S. Medici, M. Peana, G. Crisponi, V. M. Nurchi, J. I. Lachowicz, M. Remelli, M. A. Zoroddu, *Coord. Chem. Rev.* **2016**, *327*, 349–359; f) T. Zhang, H. Q. Huang, H. X. Mei, D. F. Wang, X. X. Wang, R. B. Huang, L. S. Zheng, *J. Mol. Struct.* **2015**, *1100*, 237–244; g) H. Y. Bai, J. Yang, B. Liu, J. F. Ma, W. Q. Kan, Y. Y. Liu, Y. Y. Liu, *CrystEngComm* **2011**, *13*, 5877–5884.

[3] a) P. Pyykkö, *Chem. Rev.* **1997**, *97*, 597–636; b) K. M. Merz, R. Hoffmann, *Inorg. Chem.* **1988**, *27*, 2120–2127; c) P. K. Mehrotra, R. Hoffmann, *Inorg. Chem.* **1978**, *17*, 2187–2189; d) A. Dedieu, R. Hoffmann, *J. Am. Chem. Soc.* **1978**, *100*, 2074–2079.

[4] a) A. Caballero-Muñoz, J. M. Guevara-Vela, A. Fernandez-Alarcon, M. A. Valentin-Rodriguez, M. Flores-Álamo, T. Rocha-Rinza, H. Torrens, G. Moreno-Alcántar, *Eur. J. Inorg. Chem.* **2021**, 2702–2711; b) A. K. Jassal, *Inorg. Chem. Front.* **2020**, *7*, 3735–3764; c) G. X. Jin, G. Y. Zhu, Y. Y. Sun, Q. X. Shi, L. P. Liang, H. Y. Wang, X. W. Wu, J. P. Ma, *Inorg. Chem.* **2019**, *58*, 2916–2920; d) J. M. Wang, H. M. Liu, *J. Mol. Struct.* **2018**, *1173*, 833–836; e) H. Schmidbaur, A. Schier, *Angew. Chem. Int. Ed.* **2015**, *54*, 746–784; *Angew. Chem.* **2015**, *127*, 756–797; f) C. R. Kim, J. Ahn, T. H. Noh, O. S. Jung, *Polyhedron* **2010**, *29*, 823–826; g) C. W. Kim, C. R. Kim, T. H. Noh, O. S. Jung, *Bull. Korean Chem. Soc.* **2009**, *30*, 2341–2344; h) X. D. Zheng, L. Jiang, X. L. Feng, T. B. Lu, *Inorg. Chem.* **2008**, *47*, 10858–10865.

[5] a) S. M. Soliman, Y. N. Mabkhot, J. H. Albering, *J. Chem. Crystallogr.* **2020**, *50*, 52–61; b) A. G. Young, L. R. Hanton, *Coord. Chem. Rev.* **2008**, *252*, 1346–1386; c) F. Hung-Low, K. K. Klausmeyer, *Inorg. Chim. Acta* **2008**, *361*, 1298–1310; d) A. N. Khlobystov, A. J. Blake, N. R. Champness, D. A. Lemenovskii, A. G. Majouga, N. V. Zyk, M. Schroder, *Coord. Chem. Rev.* **2001**, *222*, 155–192.

[6] a) F. L. Zhang, L. Tian, L. F. Qin, J. Q. Chen, Z. J. Li, X. H. Ren, Z. G. Gu, *Polyhedron* **2016**, *104*, 9–16; b) S. Welsch, C. Lescop, M. Scheer, R. Reau, *Inorg. Chem.* **2008**, *47*, 8592–8594; c) Z. P. Deng, L. N. Zhu, S. Gao, L. H. Huo, S. W. Ng, *Cryst. Growth Des.* **2008**, *8*, 3277–3284; d) B. L. Schottel, H. T. Chifotides, M. Shatruk, A. Chouai, L. M. Perez, J. Bacsa, K. R. Dunbar, *J. Am. Chem. Soc.* **2006**, *128*, 5895–5912.

[7] a) P. Weis, C. Hettich, D. Kratzert, I. Krossing, *Eur. J. Inorg. Chem.* **2019**, 1657–1668; b) R. Hamze, S. Y. Shi, S. C. Kapper, D. S. M. Ravinson, L. Estergreen, M. C. Jung, A. C. Tadle, R. Haiges, P. I. Djurovich, J. L. Peltier, R. Jazzar, G. Bertrand, S. E. Bradforth, M. E. Thompson, *J. Am. Chem. Soc.* **2019**, *141*, 10118–10118; c) S. Evariste, A. M. Khalil, M. E. Moussa, A. K. W. Chan, E. Y. H. Hong, H. L. Wong, B. Le Guennic, G. Calvez, K. Costuas, V. W. W. Yam, C. Lescop, *J. Am. Chem. Soc.* **2018**, *140*, 12521–12526; d) D. Yadav, R. K. Siwatch, G. Mukherjee, G. Rajaraman, S. Nagendran, *Inorg. Chem.* **2014**, *53*, 10054–10059; e) A. Serpe, F. Artizzu, L. Marchio, M. L. Mercuri, L. Pilia, P. Deplano, *Cryst. Growth Des.* **2011**, *11*, 1278–1286; f) F. A. Cotton, E. V. Dikarev, M. A. Petrukhina, *Angew. Chem. Int. Ed.* **2001**, *40*, 1521–1523; *Angew. Chem.* **2001**, *113*, 1569–1571.

[8] a) K. Škoch, I. Císařová, P. Štěpnička, *Inorg. Chem. Commun.* **2017**, *84*, 234–236; b) K. Škoch, I. Císařová, J. Schulz, U. Siemeling, P. Štěpnička, *Dalton Trans.* **2017**, *46*, 10339–10354; c) K. Škoch, F. Uhlik, I. Císařová, P. Štěpnička, *Dalton Trans.* **2016**, *45*, 10655–10671.

[9] a) M. Elsayed Moussa, P. A. Shelyganov, M. Seidl, E. Peresypkina, N. Berg, R. M. Gschwind, G. Balázs, J. Schiller, M. Scheer, *Chem. Eur. J.* **2021**, *27*, 5028–5034; b) M. Elsayed Moussa, M. Fleischmann, G. Balázs, A. V. Virovets, E. Peresypkina, P. A. Shelyganov, M. Seidl, S. Reichl, M. Scheer, *Chem. Eur. J.* **2021**, *27*, 9742–9747; c) M. Elsayed Moussa, J. Schiller, E. Peresypkina, M. Seidl, G. Balázs, P. Shelyganov, M. Scheer, *Chem. Eur. J.* **2020**, *26*, 14315–14319; d) M. Scheer, *Dalton Trans.* **2008**, 4372–4386; e) L. J. Gregoriades, H. Krauss, J. Wachter, A. V. Virovets, M. Sierka, M. Scheer, *Angew. Chem. Int. Ed.* **2006**, *45*, 4189–4192; *Angew. Chem.* **2006**, *118*, 4295–4298.

[10] a) M. Elsayed Moussa, M. Fleischmann, E. V. Peresypkina, L. Dutsch, M. Seidl, G. Balazs, M. Scheer, *Eur. J. Inorg. Chem.* **2017**, 3222–3226; b) M. Scheer, L. J. Gregoriades, M. Zabel, J. Bai, I. Krossing, G. Brunklaus, H. Eckert, *Chem. Eur. J.* **2008**, *14*, 282–295.

[11] a) E. Peresypkina, K. Grill, B. Hiltl, A. V. Virovets, W. Kremer, J. Hilgert, W. Tremel, M. Scheer, *Angew. Chem. Int. Ed.* **2021**, *60*, 12132–12142; *Angew. Chem.* **2021**, *133*, 12239–12250; b) E. Peresypkina, C. Heindl, A. Virovets, H. Brake, E. Madl, M. Scheer, *Chem. Eur. J.* **2018**, *24*, 2503–2508; c) C. Heindl, E. Peresypkina, A. V. Virovets, I. S. Bushmarinov, M. G. Medvedev, B. Kramer, B. Dittrich, M. Scheer, *Angew. Chem. Int. Ed.* **2017**, *56*, 13237–13243; *Angew. Chem.* **2017**, *129*, 13420–13426; d) F. Dielmann, E. V. Peresypkina, B. Kramer, F. Hastreiter, B. P. Johnson, M. Zabel, C. Heindl, M. Scheer, *Angew. Chem. Int. Ed.* **2016**, *55*, 14833–14837; *Angew. Chem.* **2016**, *128*, 15053–15058; e) F. Dielmann, C. Heindl, F. Hastreiter, E. V. Peresypkina, A. V. Virovets, R. M. Gschwind, M. Scheer, *Angew. Chem. Int. Ed.* **2014**, *53*, 13605–13608; *Angew. Chem.* **2014**, *126*, 13823–13827; f) M. Scheer, A. Schindler, R. Merkle, B. P. Johnson, M. Linseis, R. Winter, C. E. Anson, A. V. Virovets, *J. Am. Chem. Soc.* **2007**, *129*, 13386–13387; g) J. F. Bai, A. V. Virovets, M. Scheer, *Science* **2003**, *300*, 781–783.

[12] H. Brake, E. Peresypkina, C. Heindl, A. V. Virovets, W. Kremer, M. Scheer, *Chem. Sci.* **2019**, *10*, 2940–2944.

[13] S. Welsch, C. Groger, M. Sierka, M. Scheer, *Angew. Chem. Int. Ed.* **2011**, *50*, 1435–1438; *Angew. Chem.* **2011**, *123*, 1471–1474.

[14] a) E. Peresypkina, M. Bielmeier, A. Virovets, M. Scheer, *Chem. Sci.* **2020**, *11*, 9067–9071; b) C. Heindl, E. V. Peresypkina, D. Ludeker, G. Brunklaus, A. V. Virovets, M. Scheer, *Chem. Eur. J.* **2016**, *22*, 2599–2604; c) M. Fleischmann, S. Welsch, E. V. Peresypkina, A. V. Virovets, M. Scheer, *Chem. Eur. J.* **2015**, *21*, 14332–14336; d) M. Fleischmann, S. Welsch, H. Krauss, M. Schmidt, M. Bodensteiner, E. V. Peresypkina, M. Sierka, C. Groger, M. Scheer, *Chem. Eur. J.* **2014**, *20*, 3759–3768; e) H. Krauss, G. Balazs, M. Bodensteiner, M. Scheer, *Chem. Sci.* **2010**, *1*, 337–342; f) M. Scheer, L. J. Gregoriades, A. V. Virovets, W. Kunz, R. Neueder, I. Krossing, *Angew. Chem. Int. Ed.* **2006**, *45*, 5689–5693; *Angew. Chem.* **2006**, *118*, 5818–5822; g) J. F. Bai, A. V. Virovets, M. Scheer, *Angew. Chem. Int. Ed.* **2002**, *41*, 1737–1740; *Angew. Chem.* **2002**, *114*, 1808–1811.

[15] O. J. Scherer, H. Sitzmann, G. Wolmershäuser, *J. Organomet. Chem.* **1984**, *268*, C9–C12.

[16] P. J. Sullivan, A. L. Rheingold, *Organometallics* **1982**, *1*, 1547–1549.

[17] a) M. Elsayed Moussa, E. Peresypkina, A. V. Virovets, D. Venus, G. Balazs, M. Scheer, *CrystEngComm* **2018**, *20*, 7417–7422; b) B. Attenberger, S. Welsch, M. Zabel, E. Peresypkina, M. Scheer, *Angew. Chem. Int. Ed.* **2011**, *50*, 11516–11519; *Angew. Chem.* **2011**, *123*, 11718–11722.

[18] J. R. Harper, A. L. Rheingold, *J. Organomet. Chem.* **1990**, *390*, C36–C38.

[19] a) M. Fleischmann, J. S. Jones, G. Balazs, F. P. Gabbai, M. Scheer, *Dalton Trans.* **2016**, *45*, 13742–13749; b) H. V. Ly, M. Parvez, R. Roesler, *Inorg. Chem.* **2006**, *45*, 345–351.

[20] a) D. Fenske, A. Rothenberger, S. Wieber, *Eur. J. Inorg. Chem.* **2007**, 648–651; b) M. F. Davis, M. Jura, W. Levason, G. Reid, M. Webster, *J. Organomet. Chem.* **2007**, *692*, 5589–5597.

[21] V. R. Bojan, E. J. Fernandez, A. Laguna, J. M. Lopez-De-Luzuriaga, M. Monge, M. E. Olmos, C. Silvestru, *J. Am. Chem. Soc.* **2005**, *127*, 11564–11565.

[22] L. Dütsch, C. Riesinger, G. Balazs, M. Scheer, *Chem. Eur. J.* **2021**, *27*, 8804–8810.

[23] L. Dütsch, M. Fleischmann, S. Welsch, G. Balazs, W. Kremer, M. Scheer, *Angew. Chem. Int. Ed.* **2018**, *57*, 3256–3261; *Angew. Chem.* **2018**, *130*, 3311–3317.

[24] a) J. Burt, W. Levason, G. Reid, *Coord. Chem. Rev.* **2014**, *260*, 65–115; b) H. Werner, *Angew. Chem. Int. Ed.* **2004**, *43*, 938–954; *Angew. Chem.* **2004**, *116*, 956–972; c) W. Levason, M. L. Matthews, G. Reid, M. Webster, *Dalton Trans.* **2004**, 51–58; d) E. Bleuel, O. Gevert, M. Laubender, H. Werner, *Organometallics* **2000**, *19*, 3109–3114; e) O. F. Wendt, L. I. Elding, *J. Chem. Soc. Dalton Trans.* **1997**, 4725–4731.

[25] J. D. Chai, M. Head-Gordon, *Phys. Chem. Chem. Phys.* **2008**, *10*, 6615–6620.

[26] C. R. Groom, I. J. Bruno, M. P. Lightfoot, S. C. Ward, *Acta Crystallogr. Sect. B* **2016**, *72*, 171–179.

[27] The indicated formula corresponds to the main component of the disordered cationic core of **6**. Due to strong disorders, for some components the connectivity of Ag^I ions could not be elucidated without doubts. For more details see Supporting Information.

[28] a) P. J. Stephens, F. J. Devlin, C. F. Chabalowski, M. J. Frisch, *J. Phys. Chem.* **1994**, *98*, 11623–11627; b) A. D. Becke, *J. Chem. Phys.* **1993**, *98*, 5648–5652; c) C. T. Lee, W. T. Yang, R. G. Parr, *Phys. Rev. B* **1988**, *37*, 785–789; d) S. H. Vosko, L. Wilk, M. Nusair, *Can. J. Phys.* **1980**, *58*, 1200–1211.

[29] a) F. Weigend, *Phys. Chem. Chem. Phys.* **2006**, *8*, 1057–1065; b) F. Weigend, R. Ahlrichs, *Phys. Chem. Chem. Phys.* **2005**, *7*, 3297–3305.

[30] Since the cationic parts of monocationic SCCs **1** and **4**, dicationic SCCs **2**, **5**, **7–9** and tetracationic SCCs **3**, **10** are similar and DFT calculations do not account for the anionic part, calculations have only been performed for one structure of each type.

[31] T. A. Manz, *RSC Adv.* **2017**, *7*, 45552–45581.

[32] One of advantages of the DDEC approach is that it provides fairly consistent results across different quantum chemistry methods (on contrary to, for example, quite popular NBO-based Wiberg Bond Index).

[33] A. D. Becke, *Phys. Rev. A* **1988**, *38*, 3098–3100.

[34] a) M. Arıcı, O. Z. Yeşilel, Y. Yeşilöz, O. Şahin, *J. Solid State Chem.* **2014**, *220*, 70–78; b) C. Y. Chen, J. Y. Zeng, H. M. Lee, *Inorg. Chim. Acta* **2007**, *360*, 21–30.

[35] a) P. A. W. Dean, *J. Chem. Educ.* **2014**, *91*, 154–157; b) G. P. Schiemenz, *Z. Naturforsch. B* **2007**, *62*, 235–243.

[36] a) J. I. Ward, M. Roxburgh, L. R. Hanton, D. A. McMorran, *Inorg. Chem. Commun.* **2018**, *87*, 44–48; b) A. Terrón, B. Moreno-Vachiano, A. Bauza, A. Garcia-Raso, J. J. Fiol, M. Barcelo-Oliver, E. Molins, A. Frontera, *Chem. Eur. J.* **2017**, *23*, 2103–2108; c) G. Lamming, J. Kolokotroni, T. Harrison, T. J. Penfold, W. Clegg, P. G. Waddell, M. R. Probert, A. Houlton, *Cryst. Growth Des.* **2017**, *17*, 5753–5763; d) A. A. Mohamed, L. M. Perez, J. P. Fackler, *Inorg. Chim. Acta* **2005**, *358*, 1657–1662.

[37] T. Lu, Q. Chen, *Chem. Methods* **2021**, *1*, 231–239.

[38] T. Lu, F. W. Chen, *J. Comput. Chem.* **2012**, *33*, 580–592.

[39] M. P. Mitoraj, A. Michalak, T. Ziegler, *J. Chem. Theory Comput.* **2009**, *5*, 962–975.

[40] R. F. W. Bader, H. Essen, *J. Chem. Phys.* **1984**, *80*, 1943–1960.

[41] The chloride anion presumably comes from dichloromethane solvent upon ionization within the ESI-MS spectrometer.

[42] The monocationic fragments containing more Ag^I ions observed in the ESI-MS spectra of synthesized compounds are ions pairs; the total charge of Ag^I is reduced to one by the presence of one or two counterions.

[43] We assume that Ag^I ion in species $[Ag\mathbf{C}]^+$ coordinate some solvent molecules due to highly unsaturated character of the metal ion.

[44] N. Reinfandt, C. Schoo, L. Dutsch, R. Koppe, S. N. Konchenko, M. Scheer, P. W. Roesky, *Chem. Eur. J.* **2021**, *27*, 3974–3978.

[45] Deposition Numbers 2207717 (for **1**), 2207718 (for **2**), 22077119 (for **3**), 2207720 (for **4**), 2207721 (for **5**), 2207722 (for **6**), 2207723 (for **7**), 2207724 (for **8**), 2207725 (for **9**), 2207726 (for **10**), 2207727 (for **11**), 2207728 (for **12**) contains the supplementary crystallographic data for this paper. These data are provided free of charge by the joint Cambridge Crystallographic Data Centre and Fachinformationszentrum Karlsruhe Access Structures service.

Manuscript received: October 24, 2022
Accepted manuscript online: December 5, 2022
Version of record online: January 11, 2023